Chapter 2

Modeling of *Leishmania donovani* citrate synthase and virtual screening of compounds using different databases

Abstract

Leishmaniasis, a neglected tropical parasitic disease caused by various species of the protozoan parasite Leishmania, poses a significant global health threat. Current treatments suffer from host toxicity and drug resistance, underscoring the urgent need for novel antileishmanial drugs. One promising target is the citrate synthase of Leishmania (Ld Citrate synthase), pivotal in carbon metabolism and essential for the parasite's survival and pathogenicity in mammalian hosts. Notably, this enzyme differs significantly in sequence and structure from its human counterpart. In this study, we constructed a model of Ld citrate synthase and conducted molecular docking, molecular dynamic simulation, MM-PBSA analysis, and pharmacokinetics studies using FDA-approved drugs from various databases. Five ligands—Vorapaxar, Bazedoxifene, Imatinib, Amyral, and Abemaciclib—were selected based on their differential binding energy compared to human citrate synthase, robust binding scores, and stable interactions with the protein's active site. These ligands adhere to Lipinski's rule of five and exhibit favorable characteristics in ADMET analysis, including absorption, solubility, permeability, distribution, metabolism, and minimal toxicity. Consequently, these ligands emerge as promising lead compounds for targeting Ld Citrate synthase, offering potential as drug candidates against Leishmaniasis.

Keywords: Leishmaniasis, Citrate synthase, Molecular docking, Md Simulation, ADMET

Part of the chapter has been published in the **Journal of Cellular Biochemistry**, 2023, 124, 1404-1422, and the Journal of Molecular Structure, 2024, 1295, 136556.

2.1 Introduction

Leishmaniasis, a parasitic disease caused by more than 20 distinct species of leishmania. It is a poverty-associated disease that basically affects the poorest of the poor, mainly in developing countries. It is of three types, but visceral leishmaniasis is a more severe one; if left untreated, it can cause death. This parasite exists in two morphological forms: the promastigote form, which occurs in sand flies and is transmitted to humans by the bite of infected leishmania species, and the amastigote form, which is found in human during infection [Singh et al., 2012], [Raj et al., 2020]. Annually, there are two million people affected by this disease in 350 million residing population of tropical and subtropical countries, and approximately 30000 deaths occur, which is considered the second leading cause of death due to parasitic infection [Silva et al., 2020]. There is no vaccine available against this disease; the whole treatment depends on chemotherapy. These options also have several drawbacks, such as parasite resistance, highly toxic side effects, painful administration routes, and prohibitive costs [Raj et al., 2020]. Therefore, there is an urgent requirement to find or design some new treatment options.

To propel the advancement of new drug development, it is imperative to focus on the life cycle of leishmania, particularly the amastigote stage and its adaptive mechanisms. Central to this process is citrate synthase, the initial enzyme in the TCA cycle responsible for catalyzing the conversion of oxaloacetate and acetyl-CoA into citrate, thereby facilitating the continuation of the TCA cycle. This cycle generates crucial molecules such as glutamate, glutamine, and aspartate, vital for synthesizing nucleotides, thiols, and amino sugars essential for parasite growth and survival (Saunders et al., 2010). Moreover, the TCA cycle contributes to the generation of reducing equivalents for the respiratory complexes. Excess citrate in the TCA cycle is transported to the cytoplasm via the mitochondrial citrate carrier (CIC) and converted by citrate lyase into acetyl-CoA and oxaloacetate. Malate, produced in the cytoplasm from oxaloacetate by malate dehydrogenase, is transported back to the mitochondria using the

same carrier. Acetyl-CoA is then utilized in fatty acid and cholesterol synthesis, serving as energy and structural components (Costa et al., 2011). Beyond its functional significance, citrate synthase exhibits substantial structural and sequence disparities compared to the human citrate synthase enzyme.

Due to their quick and efficient drug development methods, the drug repurposing technique has emerged as an interesting area of research for finding prospective lead compounds from approved medications against the drug targets of various diseases [Wang et al., 2019] [Gagic et al., 2020]. In these methods, *in silico* methods are demonstrated to be a practical tool for screening larger compound databases and have emerged as a feasible time and cost-effective drug development strategy.

In this study, we employed modeling of citrate synthase and an in-silico drug repurposing approach based on molecular docking, MD simulation, and MMPBSA analysis to find a possible inhibitor against the *L. donovani* citrate synthase (LdCS) enzyme in an FDA-approved compounds.

2.2 Materials & Methods

2.2.1 Modelling of Citrate synthase and its validation

The Ld citrate synthase amino acid sequence was taken from the NCBI protein database (XP_003860083.1), and its 3D structure was built using the I-TASSER server [Yang and Zhang, 2015]. This server constructs a model based on multiple threading alignments of the sequences and Z score. In this process, the alignment and assembly of all fragments were done using the conformational constraints of the template structure, and then, based on the relative cluster of the structure density and consensus significance, the structure of the predicted model was matched with the known protein structure from RCSB PDB, and C-score was assigned. Finally, using this C score, the best model was selected for further studies [Singh et al., 2015]; [Yang and Zhang, 2015]; [Zhang et al., 2017]. The energy minimization of the best-modeled

structure was done using the Swiss-PDB Viewer program. The actual position and nature of amino acid and phi and psi angle inspection within the modeled structure were predicted by Ramachandran plot via RAMPAGE [Lovell et al., 2003]; [Rana et al., 2017]. Validation of the overall quality of the chosen model was done by the ProSA program [Wiederstein and Sippl, 2007].

2.2.2 Ligand Preparation

The FDA-approved ligands were retrieved from the subset of the ZINC 15 database in spatial data file (SDF) format and then converted into mol2 format using Open Babel [Boyle et al., 2011]. Mol2 format was further converted into PDBQT format with the help of the graphical user interface version of Raccoon.

2.2.3 Active site prediction

The active site is the ligand coordinates in the target protein grid where ligands bind and become functional. The Ld citrate synthase protein's active site and binding pocket were analyzed by Phyre2 [Kelley et al., 2015] and 3D Ligand Site virtual tools [Wass et al., 2010].

2.2.4 Molecular docking and its analysis

The molecular docking and interaction studies were carried out with the help of AutoDock version 4.2 [Morris et al., 2010]. In this study, ligands were considered conformationally flexible, and protein as a rigid structure. The AMBER force field was used for the estimation of the free binding energy of the ligand to its target [Verma et al., 2012]. The selected Ld citrate synthase protein model was converted into PDBQT format with the help of the MGLTools-1.5.6 software of AutoDock. Molecular screening of all ligands was done by using Raccoon and MGL Tools-1.5.6 software of AutoDock for docking. A grid box was set to cover a residue present in the binding cavity and act as a docking target site. It had X, Y, and Z coordinates of 72 x 62 x 44 and 0.375 Å grid spacing [Vargas et al., 2018]. Besides electrostatic and desolvation maps, grid maps were also generated, representing all available atom types in

protein and probable atom types in the ligand [Cosconati et al., 2010]. The docking simulation used a Lamarckian genetic algorithm (LGA), which had a property of both genetic and local search algorithms [Morris et al., 2010]; [Chakraborty et al., 2013]. The docking simulation was performed for 1055 natural and 1565 FDA-approved ligands. Ligands that showed free binding energy less than equal to -9 kcal/mol were selected for further study [Chakraborty et al., 2013]. The binding interaction of ligand and Ld citrate synthase protein was analyzed using a Discovery studio visualizer.

2.2.5 ADME analysis

Most of the drug failures occur in clinical trials due to their poor pharmacokinetics and toxicity properties. Hence, ADMET analysis has become essential for selecting drugs before an expensive experimental procedure of clinical trials [Puratchikody et al., 2016]. Selected ligands in the SMILES format were submitted to the Swiss ADME server [Daina et al., 2017] and the pkCSM server [Pires et al., 2015a]. The Swiss ADME server predicted Lipinski's rule of 5 for these ligands. The orally active drugs should satisfy at least four criteria out of five. The pkCSM server did an ADMET analysis of these ligands. This analysis is essential for the pharmacokinetic study of a drug molecule. Miltefosine is an orally administered anti-leishmanial drug used as a control to understand and interpret the result with selected ligands [Sangshetti et al., 2015] [Dhorajiwala et al., 2019].

2.2.6 Molecular dynamic simulation and its analysis

The molecular dynamic simulation of the LdCS as apoprotein and the above-selected ligands was carried out for 100 ns by GROMACS v 2018.8 software using GROMOS96 54a7 force field [Schmid et al., 2011]. The parameter and topology file of the ligands were generated using PRODRG 2.5 and Automated Topology Builder (ATB v 3.0) server) [Schüttelkopf and Van Aalten, 2004]; [Malde et al., 2011]. The solvation of protein and ligand complex was done with SPC water molecules in a dodecahedral box with a 1.0 nm distance between the box edge and

protein surfaces and neutralization using appropriate ions. Energy minimization of the system was done using the steepest descent method with the maximum step set of 50000 and a tolerance of 1000 KJ mol^{-1} nm^{-1}. The equilibrations of the system were done with NVT and NPT steps. The NVT step was carried out for 500 ps with a modified Berendsen thermostat at 310 K and 0.1 ps time. In contrast, the NPT was carried out for 1ns with Parrinello-Rahman pressure coupling at 1 bar with isothermal compressibility of 4.5 X 10^{-5} bar^{-1} and a time constant of 2.0 ps. The PME coulomb type was used for long-range electrostatics interaction with 1.0 nm cut-off and 0.16 Fourier spacing [Borkotoky and Banerjee, 2020]. The inbuilt utilities of Gromacs' were used for analysis of Root Mean Square Deviation (RMSD), Root Mean Square Fluctuation (RMSF), Radius of Gyration (Rg), and Number of Hydrogen Bonds (H-bond) trajectory files. The qtgrace tool was used to produce the graph [Raj et al., 2019]. The g mmpbsa tool, a subroutine of the GROMACS and APBS62 packages, was used to determine the free binding energy of protein-ligand complexes from MD trajectories [Kumari et al., 2014]. It uses Poisson- Boltzmann (PB), an implicit solvent approach, and "Solvent Accessible Surface Area" (SASA), a non-polar solute-solvent approach, to determine the free binding energy of complexes and also free binding energy contribution of each residue. For the calculation of free binding energy, 201 snapshots were captured from the final 20 ns of the trajectories.

2.3 Results

2.3.1 Modelled Structure Prediction and its Validation

The 3D structure of the Ld citrate synthase model was built using the I-TASSER server, and its quality was predicted based on their template selection, Z score, C score, and interaction with their substrate. The best model is shown in Figure 2.1(A), which is further validated by the PROCHECK, RAMPAGE, and ProSA server. The PROCHECK server validated the model and showed that it consists of alpha-helix and a few flexible loops. The RAMPAGE server has

drawn the Ramachandran plot of the predicted model, as shown in Figure 2.1 (B), to verify the torsion angles (Φ, φ) of backbone carbon. It was observed from the plot that 90.2% of the residues were present in the favored region, 8.8% in the allowed region, and 1.0% residues, i.e., only three amino acids in the disallowed region. The ProSA-web server further verified the selected model based on the Z score and energy graph, representing the overall protein structure quality. The Z score of the selected model was -5.59, which was represented as a dark black point in the X-ray region of the graph, as shown in Figure 2.1 (C). This score was present in the acceptable range of -10 to 10 [Gupta et al., 2013]. There has been a report that the Z score value is dependent on the length of the protein, and a negative value is suitable for a model. The local model quality was plotted with energy vs. amino acid sequence position, and the plot was shown in Figure 2.1 (D). The positive value represents the problematic part of the input structure [Maganti et al., 2010].

3.3.2 Active Site Prediction

The active site of LdCS was predicted by Phyre2, 3D Ligand site, and ITASSER server. These amino acids, Arg 49, His245, Val250, Ser251, Pro279, Leu280, His281, and Ala284, were present in the active site. The binding pocket of LdCS was formed with these Tyr238, Val241, His242, Ala243, Asp244, His245, Glu246, Gly247, Asn249, Val250, Ser251, Ala252, Thr255, Thr256, Ala259, Leu262, Ser263, Asp264, Pro265, Ala268, Phe269, Gly272, Leu273, Leu276, His281, Gly282, Ala284, and Asn285 amino acids whereas the binding pocket of Human Citrate synthase (HsCS) was formed with Tyr 258, Ilu 261, His 262, Ser 263, Asp 264, His 265, Glu 266, Gly 267, Asn 269, Val 270, Ser 271, Ala 272, Ser 275, His 276, Gly 279, Leu 282, Ser 283, Asp 284, Pro 285, Ser 288, Phe 289, Ala 292, Met 293, Leu 296, His 301, Gly 302, Asn 305, Arg 356, Phe 424, Arg 428 amino acids as shown in Figure 2.2 (A). The majority of amino acids present in the binding pocket were hydrophobic. The multiple sequence alignment of all Leishmania species citrate synthase protein was done, and all the predicted amino acids

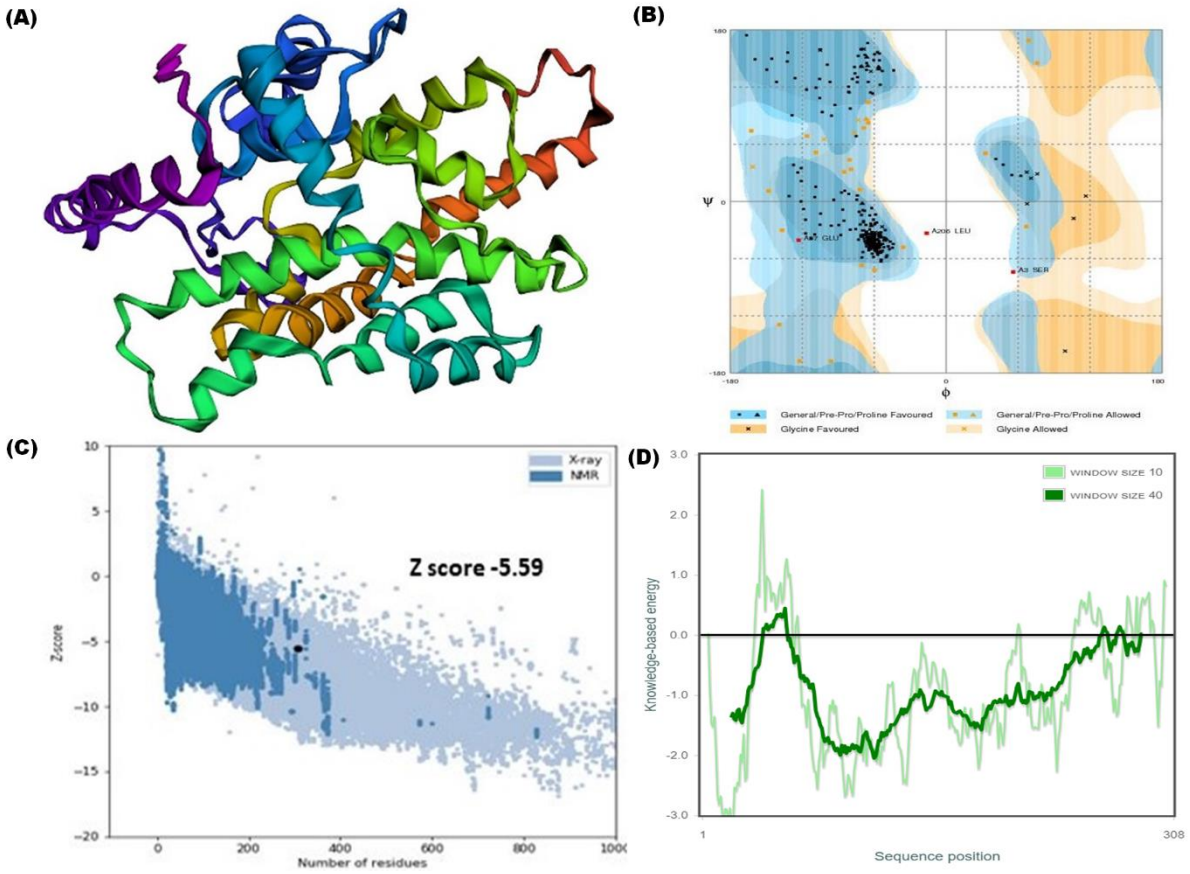

Figure 2.1: *Leishmania donovani* Citrate synthase (LdCS) model and its validation using PROCHECK, RAMPAGE, and ProSA server. (A) The 3D structure of the LdCS model is modeled through the I-TASSER server and validated by PROCHECK. **(B)** Ramachandran plot analysis of the LdCS model indicates various residues in favored, allowed, and outlier regions. **(C)** Stereochemical validation of the LdCS model in terms of Z-score obtained from the ProSA server. The Z-score is highlighted as a black dot in the plot, which contains the Z-score of all experimentally determined protein chains currently available in the Protein Data Bank. The group of structures from different sources (X-ray and NMR) is distinguished by different colors, i.e., light and dark blue. **(D)** A plot of single residues was obtained through the ProSA server, where window sizes of 40 and 10 residues were distinguished by dark and light green lines.

by the above method were present in the conserved region of the sequence. The binding site residues containing *Leishmania donovani* citrate synthase (LdCS) structure and Human Citrate synthase (HsCS) structure were superimposed, and in the superimposed region, there were a lot of differences in binding site residues between LdCS and HsCS observed as shown in Figure 2.2 (B).

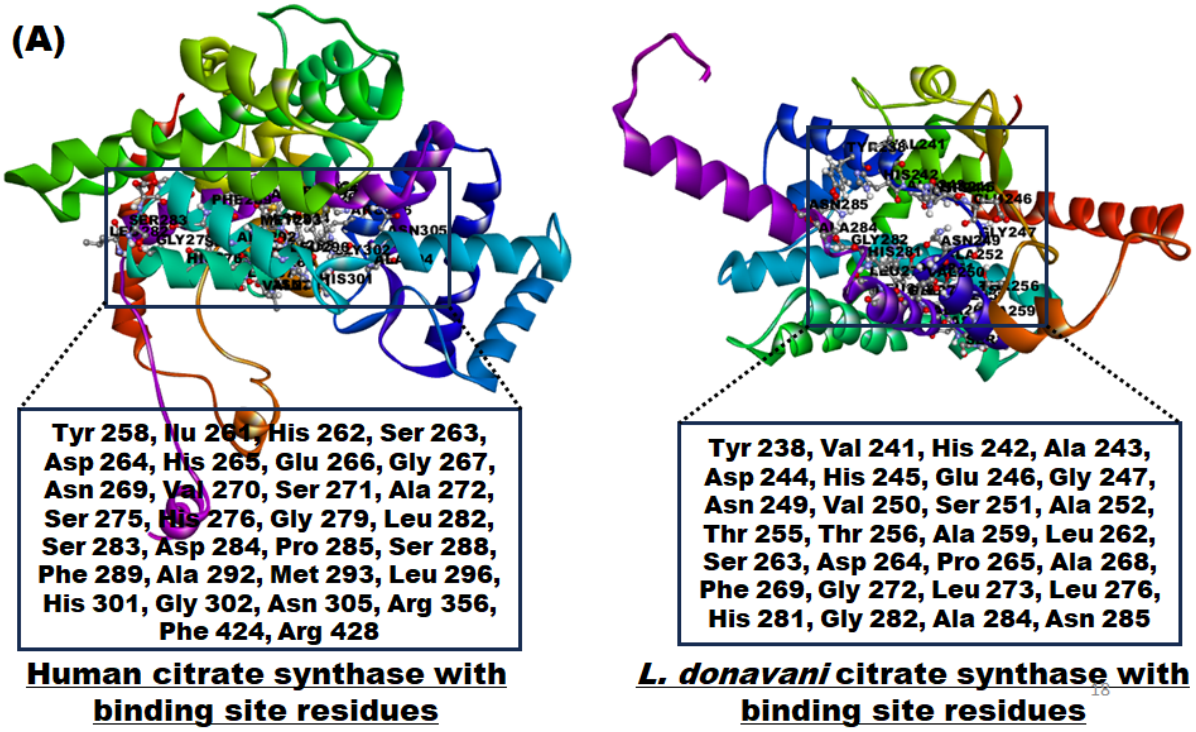

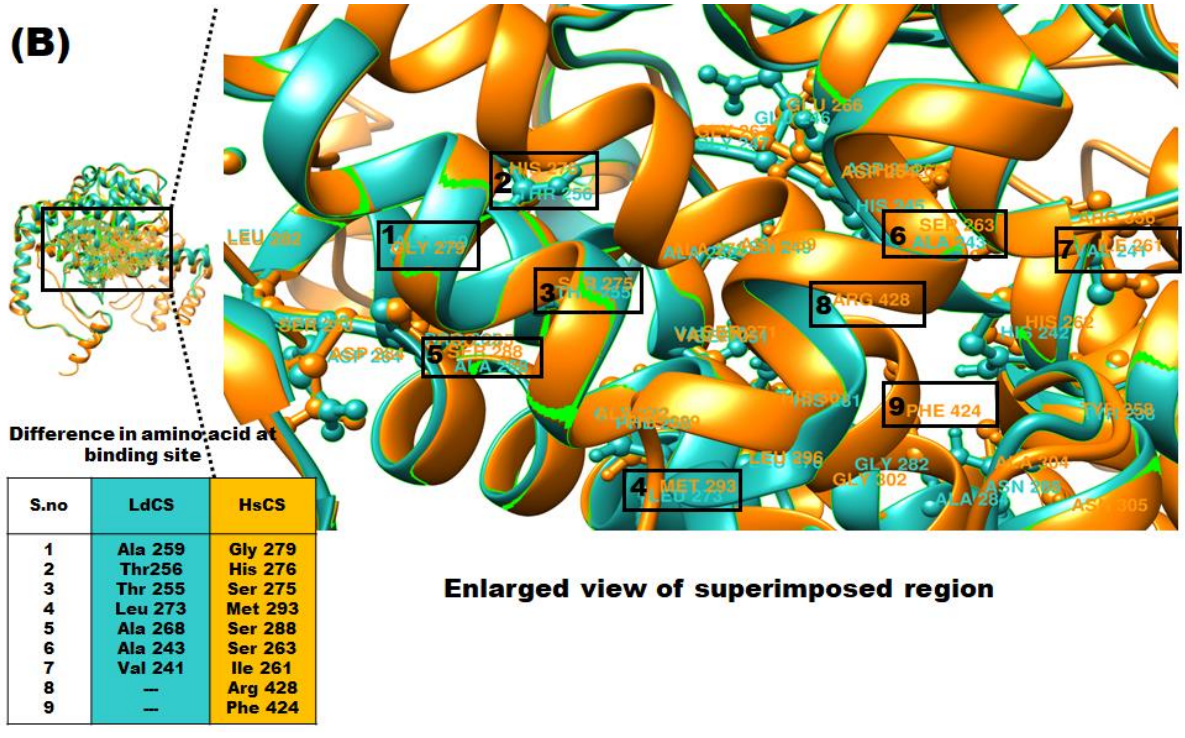

Figure 2.2: Binding site residues of LdCS and HsCS. (A) Structure of LdCS and HsCS with binding site residues and (B) Superimposed region of the binding site of LdCS and HsCS and its enlarged view. Here, LdCS and its binding site residues are represented by Tile color, and HsCS and its binding site residues are represented by orange.

2.3.3 *In Silico* Studies with Natural Compound Database

2.3.3.1 Molecular docking and its analysis

Molecular docking is a highly convenient and widely used method in computer-aided drug discovery. It helps identify lead molecules from large compound libraries that can bind to protein macromolecules with good binding energy and form stable complexes. AutoDock Vina is an open-source program for drug discovery with multiple properties, i.e., multi-core capability, high performance with enhanced accuracy, and ease to use [Herowati and Widodo, 2014]. In this study, Staurosporine, Solasodine, Cromolyn, and Oxetacine were selected from 1055 compounds based on binding energy and interaction with the active site of LdCS, as shown in Table 2.1. The binding site of LdCS contains these Tyr 238, Val 241, His 242, Ala 243, Asp 244, His 245, Glu 246, Gly 247, Asn 249, Val 250, Ser 251, Ala252, Thr 255, Thr 256, Ala 259, Leu 262, Ser 263, Asp 264, Pro 265, Ala 268, Phe 269, Gly 272, Leu 273, Leu 276, His 281, Gly 282, Ala 284 and Asn 285 amino acid.

Table 2.1: Natural compound showing free binding energy (kcal/mol) with LdCS & HsCS and its current application.

Compound Name	Free Binding Energy with HSCS (kcal/mol)	Free Binding Energy with LdCS (kcal/mol)	The Difference in Free Binding Energy (kcal/mol)	Current Application
Staurosporine	-8	-10.4	2.4	Cancer
Solasodine	-8	-10.3	2.3	Contraceptive pills
Cromolyn	-6.9	-9.4	2.5	Mastocytosis
Oxetacaine	-6.8	-9.2	2.4	Antacid

In docking analysis, the binding energy of Staurosporine was found to be -10.4 kcal/mol. They showed π-alkyl, π-π T shaped and carbon-hydrogen bond interaction with Ala 243, Phe 269, Leu 185 & Asp 244, and Vander Waal interaction with Leu 239, His 242, Ser 251, Ala252, Thr 255, Leu 273 and Leu 276 as shown in Figure 2.3 (A). In Cromolyn, the binding energy was calculated as -9.4 kcal/mol. They had also shown π-π T-shaped interaction with Ser 251, π-alkyl interaction with Leu 185, and π-sigma interaction with Ala 252. They also showed Vander Waal interaction with Ala 243, Asp 244, His 245, Asn 249, Thr 255, Phe 269, Leu 273, and Leu 276, as shown in Figure 2.3 (B).

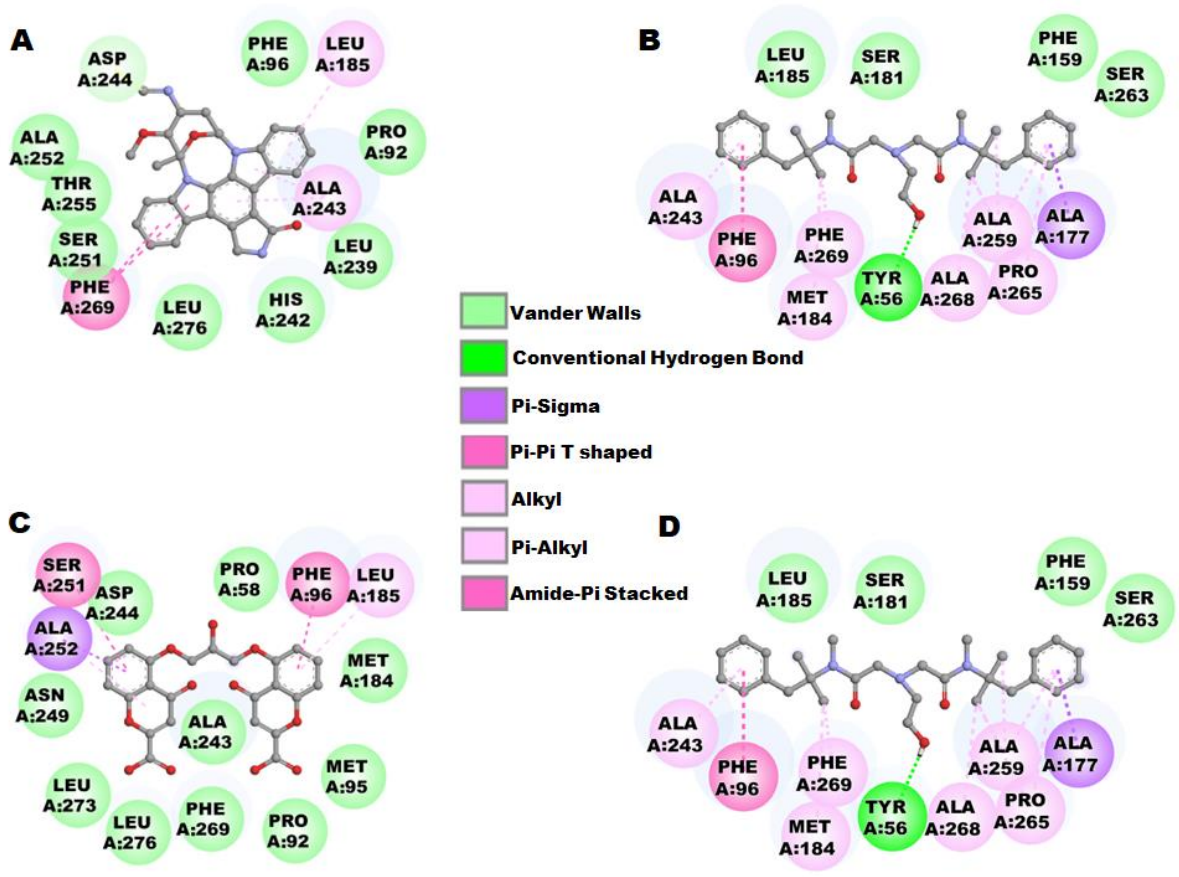

Figure 2.3: Interaction of compounds with LdCS.
2D illustration of interactions between compounds **(A)** Staurosporine, **(B)** Oxetacaine, **(C)** Solasodine, and **(D)** Cromolyn and LdCS active site residues. Different color indicates their different type of interaction. The results were visualized and produced using the Discovery Studio Visualizer software.

In Oxetacaine, the binding energy was found to be -9.2 kcal/mol. They had one Hydrogen bond with Tyr 56. They showed alkyl and π-alkyl interaction with Ala243, Ala 259, Pro 265, Ala268, and Phe 269 and Vander Waal interaction with Asp 244, Thr 255, Leu 262, and Ser 263 shown in Figure 2.3 (C). In the case of Solasodine, the binding energy was measured to be -10.3 kcal/mol. On analyzing the interaction, Val 192, Trp 216, Leu 224, Tyr 238, and Leu 239 exhibited alkyl and π-alkyl interaction, and with Phe 146, Thr 188, Thr 200, Phe 220, Phe 226, Phe 231, and Met 235 showed Vander Waal interaction as shown in Figure 2.3 (D).

3.3.3.2 Pharmacokinetics analysis

Although the selected molecules were pre-filtered using Lipinski's rule, to predict the drug-likeness of ligand molecules, the analysis of pharmacokinetics properties was required. In drug development, the lead molecule should have good absorption, distribution, metabolism, and toxicity (ADMET) properties, improving the probability of clinical success. Thus, the ADMET analysis becomes essential for developing an effective druggable molecule [Wu et al., 2020]. In this study, the pkCSM server predicts the ADMET properties of molecules based on graph-based signatures [Pires et al., 2015]. The pharmacokinetics results of all the selected natural molecules, i.e., Staurosporine, Solasodine, Cromolyn, and Oxetacaine, are shown in Table 2.2, which revealed that all the molecules were water-soluble as their values were less than five and almost equal to five. The Caco2 permeability analysis was done to check the molecules' oral absorption and transport mechanism. Staurosporine and Solasodine had high Caco2 permeability as their value was greater than 0.9, and Cromolyn and Oxetacaine had a value less than 0.9. All molecules had excellent human intestinal absorption since their values were ≥ 30% and low excretion as total clearance values (logCLtot < 2.0), indicating that all the selected molecules have good pharmacokinetics profiles for oral routes. [da Paixão and Pita, 2019]. These molecules were permeable to the skin as their values (log Kp) < -2.5 and did not show any skin sensitization properties that predict that these molecules could be used for skin-related

disease and cutaneous Leishmaniasis. P-glycoprotein is also crucial for the absorption and distribution of drugs as it acts as a biological barrier after removing drugs and xenobiotics compounds from the cells [Broni et al., 2021]. All the selected molecules were predicted as P-glycoprotein substrates. All molecules had a volume of distribution VDss < 0.71 L/kg except Solasodine, which had more than 0.71 L/kg but less than 2.8 L/kg. Thus, these molecules have a high plasma-protein binding capacity, implying a long half-life and stable efficacy [Wu et al., 2020]. The blood-brain permeability of all these compounds was low as Staurosporine and Oxetacaine had a value > -1, but Solasodine and Cromolyn had a value < -1 but < 0.3. Thus, these molecules cannot cross the blood-brain barrier and reduce the side effects and toxicity of the brain. Except, Staurosporine and Solasodine, which contain log PS value > -2, permeable to the central nervous system (CNS), other molecules such as Cromolyn and Oxetacaine are unable to penetrate CNS as their values were log PS < -3 [Pires et al., 2015]. The superfamily of cytochrome P450 mono-oxygenase (CYP) plays a crucial role in drug metabolism. It oxidizes the drugs and xenobiotics compounds and facilitates their extraction from the body [Wang et al., 2019]. Selected molecules except Oxetacaine did not inhibit CYP450. The toxicological result of the selected molecules was evaluated based on AMES toxicity, hepatotoxicity, and hERG inhibitor. The Ames prediction test indicated that, except Staurosporin, the chosen molecules were not mutagenic or carcinogenic. There were no molecules except for Staurosporin and Solasodine found, which will disrupt the liver's normal function. Inhibition of the potassium channel encoded by hERG leads to fatal ventricular arrhythmia. No molecules were found to be hERG inhibitors [da Paixão and Pita, 2019]. Altogether, the selected natural molecules, Cromolyn and Oxetacaine, do not have any pharmacological and toxicological issues. Thus, these molecules could be employed in an in-vitro experiment.

Table 2.2: Analysis of pharmacokinetics properties of ligands, i.e., Staurosporine, Solasodine, Cromolyn, and Oxetacaine, that had been predicted by the pkCSM server.

ADMET Properties	Ligand Name			
	Staurosporine	**Solasodine**	**Cromolyn**	**Oxetacaine**
Water Solubility (Log mol/L)	-3.895	-5.168	-3.07	-4.314
Caco2 permeability (Log P_{app} in 10^{-6} cm/s)	1.139	1.25	0.05	0.866
Intestinal Absorption (% absorbed)	97.545	93.875	38.615	95.319
Skin Permeability (Log Kp)	-2.735	-3.097	-2.735	-2.722
P-glycoprotein Substrate	Yes	Yes	Yes	Yes
P-glycoprotein inhibitor	Yes	Yes	No	Yes
VDss (human) (Log L/kg)	-0.593	0.762	-1.828	0.697
BBB Permeability (Log BB)	-0.151	0.203	-1.545	-0.541
CNS Permeability (Log PS)	-2	-1.834	-4.191	-2.771
CYP Substrate	Yes	Yes	No	Yes
CYP Inhibitor	No	No	No	Yes
Total Clearance (Log ml/min/kg)	1.159	0.082	0.591	0.88
AMES Toxicity	Yes	No	No	No
Max tolerated dose (human) (Log mg/kg/day)	0.335	-0.359	0.726	0.062
hERG Inhibitor	No	No	No	No
Hepatotoxicity	Yes	Yes	No	No
Skin Sensitization	No	No	No	No

Note: Water solubility < 5; Intestinal absorption > 30%; Skin permeability (log Kp) < -2.5; VDss is low if VDss < 0.71 L/kg and high if VDss > 2.81 L/kg; BBB permeable if logBB > 0.3; BBB not permeable if logBB > -1; CNS permeable if logPS > -2; CNS not permeable if logPS < -3; MRTD ≤ 0.477 log(mg/kg/day) is low while > 0.477 log(mg/kg/day) is high.

2.3.3.3 Molecular dynamic simulation and its analysis

MD simulations are performed to understand the docking complexes' flexibility and stability at certain time intervals in a hydrated environment. Accounting for the flexibility of both ligand and protein, refining docking, and estimating the ligand binding affinities [Vargas et al., 2018].

Root Mean Square Deviation (RMSD) of complexes

To understand the stability of the complexes, The RMSD of the backbone atom of Ld citrate synthase and the protein-ligand complex was estimated for 100 ns, and its plot was shown in Figure 2.4 (A). The Ld citrate synthase had RMSD 0.7 nm and showed convergence from 10 ns. The complex Staurosporine, Solasodine, and Cromolyn had RMSD 0.8 nm and showed convergence from 15 ns. The complex Oxetacaine had RMSD 1.2 nm and showed convergence from 15 ns. The RMSD plot of the ligand of complexes is shown in Figure 2.4 (B). The complex Staurosporine and Solasodine were stable from the initial and their RMSD values of 0.05 nm and 0.1 nm. The complex Cromolyn and Oxetacaine had an RMSD value of 0.3 nm, and it became stable after 50 ns and 10 ns.

Root Mean Square Fluctuation (RMSF) of complexes

The RMSF reveals the local fluctuation and flexibility of different protein regions, which might be related to crystallographic B-factors. Higher RMSF values imply more tremendous changes. The RMSF of Ld citrate synthase and all the complexes, i.e., Staurosporine, Solasodine, Cromolyn, and Oxetacaine, were analyzed, and its graph was shown in Figure 2.4 (C). The RMSF plot revealed that all complexes showed some degree of fluctuations at the N-terminal region from 25 to 50 residues and at the C-terminal region from 290 to 308. The fluctuation in the N-terminal and C-terminal regions might be due to the presence of a loop and low, stable β-sheet [Kuldeep et al., 2020]. All complexes had RMSF values of 0.5 nm in the active site region and showed meager fluctuations.

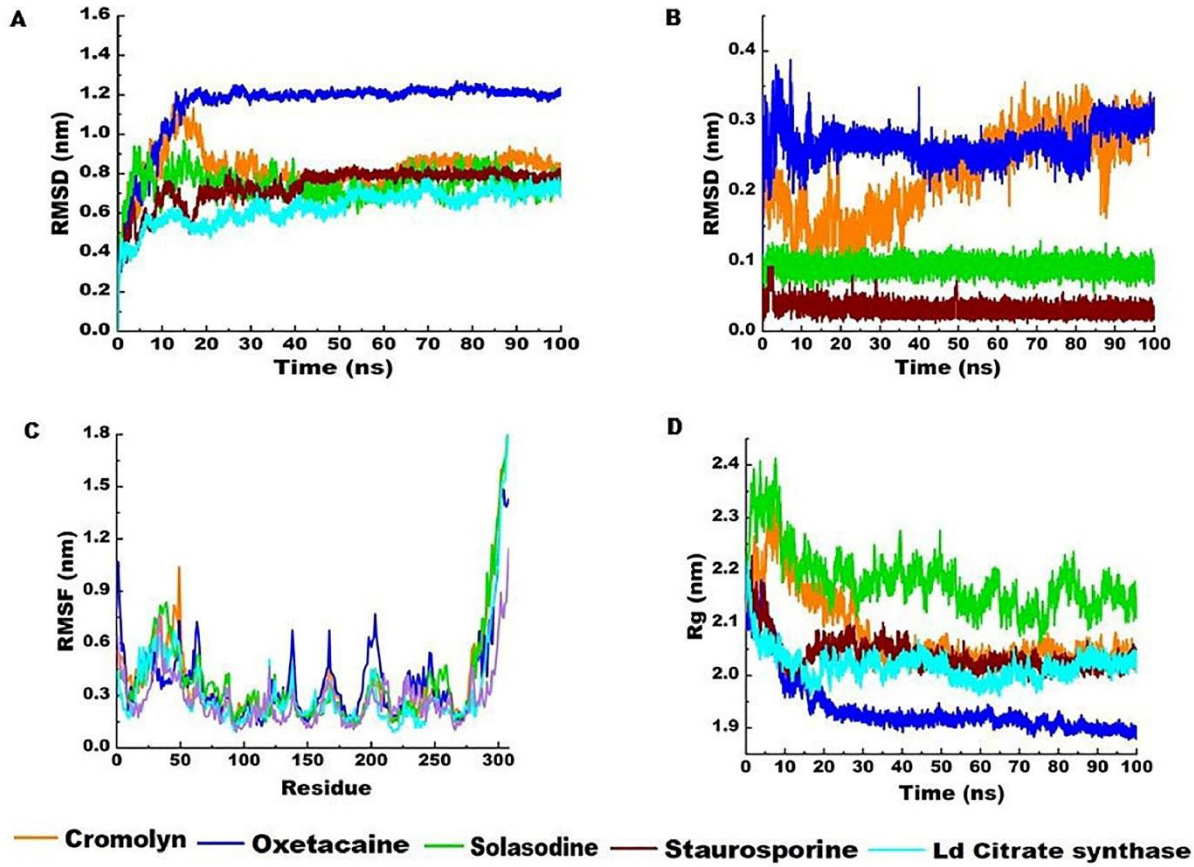

Figure 2.4: Molecular Dynamic Simulation analysis of LdCS and Complexed compounds, i.e., Cromolyn, Oxetacaine, Solasodine, and Staurosporine, which was performed for the duration of 100 ns. (A) RMSD plot of the LdCS protein's protein backbone atom and complexed compounds. **(B)** RMSD plot of Compounds complexed with LdCS protein. **(C)** RMSF plot of all 308 residues of LdCS protein and complexed compounds. **(D)** Rg plot of LdCS protein and complexed compounds. Each complex was displayed using a different color.

The Radius of Gyration (Rg) of complexes

This study inspects the protein-ligand complexes' compactness, conformation, and folding patterns in the simulation period. The introduction of a weak intermolecular bond affects the compactness and stability of the complex. The Rg of the complex is indirectly related to the compactness of the protein-ligand complex, i.e., when the Rg value increases, the compactness of the complexes decreases, and its interaction becomes weak [Liao et al., 2014]. A steady-folded protein maintains a relatively stable Rg, but its value changes over time according to protein folds and unfolds. The Rg value of Ld citrate synthase and all complexes, i.e., Staurosporine, Solasodine, Cromolyn, and Oxetacaine, was found between 1.9 to 2.25 nm and shown in Figure 2.4 (D). The Rg of Ld citrate synthase was 2.05 nm, with minimal fluctuation.

The complex Staurosporine and Cromolyn had an Rg value of 2.05 nm and became stable after 20 ns. The Rg values of Solasodine and Oxetacaine were 2.2 nm and 1.95 nm, which became stable after 15 ns. All complexes sustain a sturdy Rg value, which indicates the highly folded protein-inhibitor structure.

Hydrogen Bond Analysis of Complexes

The number of hydrogen bonds in intermolecular H-bond interaction confers the rigidity and specificity of the protein-ligand interaction [Muthuvel et al., 2018]. The number of hydrogen bond formations in complexes is shown in Figure 2.5. The maximum number of H-bonds present in Oxetacaine was four, and an average of three H-bonds. This complex had formed an H-bond with Val 241 and Thr 255. The complex Solasodine and Cromolyn contain maximum H-bonds 3 & 2 and maintain an average of up to 2. In contrast, the complex Staurosporine had a maximum H-bond one throughout the simulation period. The residue involved in H-bond formation with Solasodine was His 242 and Asn 285, whereas with Cromolyn Asp 244, His 245, Asn 249, Ser 251, Thr 255, Ser 263, Asp 264, Phe 269, Gly 272, His 281, Gly 282 and Leu 283. In the case of Staurosporine, the residue involved in H bond formation was His 242 and Ala 243.

MM/PBSA analysis

At a quantitative level, compared to other computational approaches, the simulation-based method is found to be a more accurate method for estimating ligand binding free energies. The quantification of protein-ligand affinity was done based on binding free energy calculation, which is the free energy difference between the ligand-bound and unbound state of protein and ligand [Ganesan et al., 2017]. This method was used to determine the binding free energies of all selected protein-ligand complexes, as shown in Table 2.3, based on four energy components, i.e., Vander Waal, Electrostatic, Polar Solvation, and SASA Energy. The binding free energies of complexes Oxetacaine and Solasodine were -256.968 ± 12.95 kJ/mol

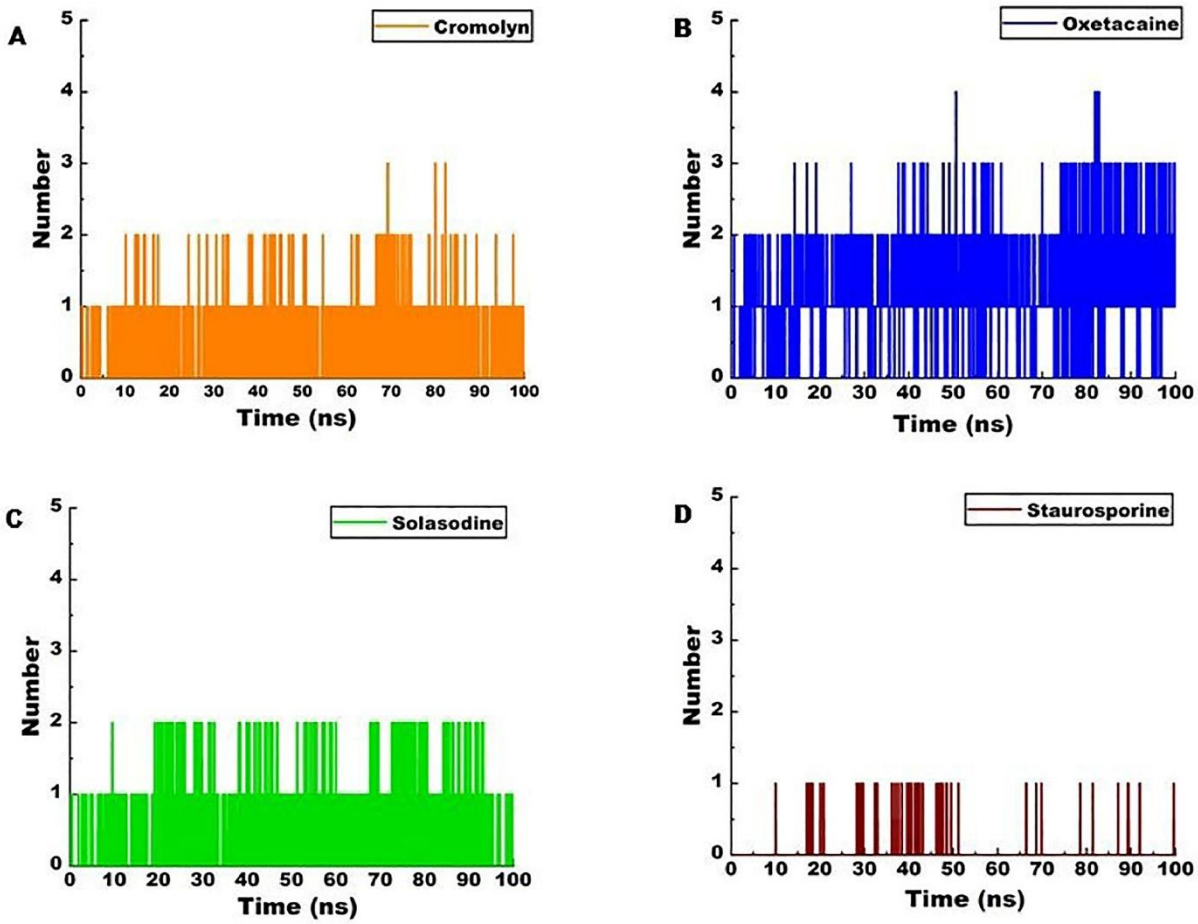

Figure 2.5: Hydrogen bond analysis.
The number of hydrogen bonds formed between LdCS protein and respective compounds in 100 ns of MD Simulation. The Average number of H-bonds formed between LdCS protein and (A) Cromolyn, (B) Oxetacaine, (C) Solasodine, and (D) Staurosporine was 2, 3, 2, and 1, respectively. Different colors had been used to represent each complex.

and -160.73 ± 55.28 kJ/mol, and other complexes like Staurosporine and Cromolyn contain binding free energies -90.97 ± 117.60 kJ/mol and -46.97 ± 103.74 kJ/mol, respectively. Based on the binding free energy calculation of complexes, the stability of Oxetacaine would be higher than those of others. The energy components which favorably involved in binding energy formation was Vander Waal Energy, Electrostatic, and SASA energy, and unfavorably, one is Polar solvation energy. In all complexes, the Vander Waals energy among all free energy components contributes to ligand binding. Based on molecular docking and MD simulation results, the binding pocket contains hydrophobic residues, which were confirmed further by the MM/PBSA analysis based on ΔE_{vdw} value, which is greater than $\Delta E_{ele.}$

Table 2.3: Calculation of average binding energy of different complexes, i.e., Staurosporine, Solasodine, Cromolyn, and Oxetacaine with Ld citrate synthase after MD simulation.

Compound Name	Vander Waal Energy (kJ/mol)	Electrostatic Energy (kJ/mol)	Polar Solvation Energy (kJ/mol)	SASA Energy (kJ/mol)	Binding Energy (kJ/mol)
Staurosporine	- 101.57	-0.96	19.72	-8.16	-90.97
Solasodine	-186.48	1.13	43.33	-18.71	-160.73
Cromolyn	-83.37	-2.44	45.41	-6.56	-46.97
Oxetacaine	-290.77	-30.19	88.91	-24.91	-256.96

Per-Residue Energy Decomposition

Although all complexes bind to the same binding pocket of the enzyme, their binding free energy is different due to each residue's binding energy contribution. The MM/PBSA analysis was also used to calculate the binding free energy of each residue. This method provides insight into the important interaction of crucial residues in free energy contribution [Broni et al., 2021]. The per-residue energy decomposition of each complex was determined and shown in Figure 2.6. From the protein-ligand interaction, residues Tyr 238, Leu 239, His 242, Ala 243, Asp 244, His 245, Asn 249, Ser 251, Ala 252, Thr 255, Phe 269, Leu 273, Leu 276, His 281, Asn 285 were deliberated as essential residues in ligand binding with LdCS binding site. The MM/PBSA decomposition computation showed that the Staurosporonin contains Tyr 238, His 242, Ala 243, Asp 244, Asp 264, Phe 269, Leu 273, and Leu 276, and Solasodine contain Tyr 238, Asp 264, Phe 269, Leu 273, Pro 279 and Ala 284 as the main contributing residue.

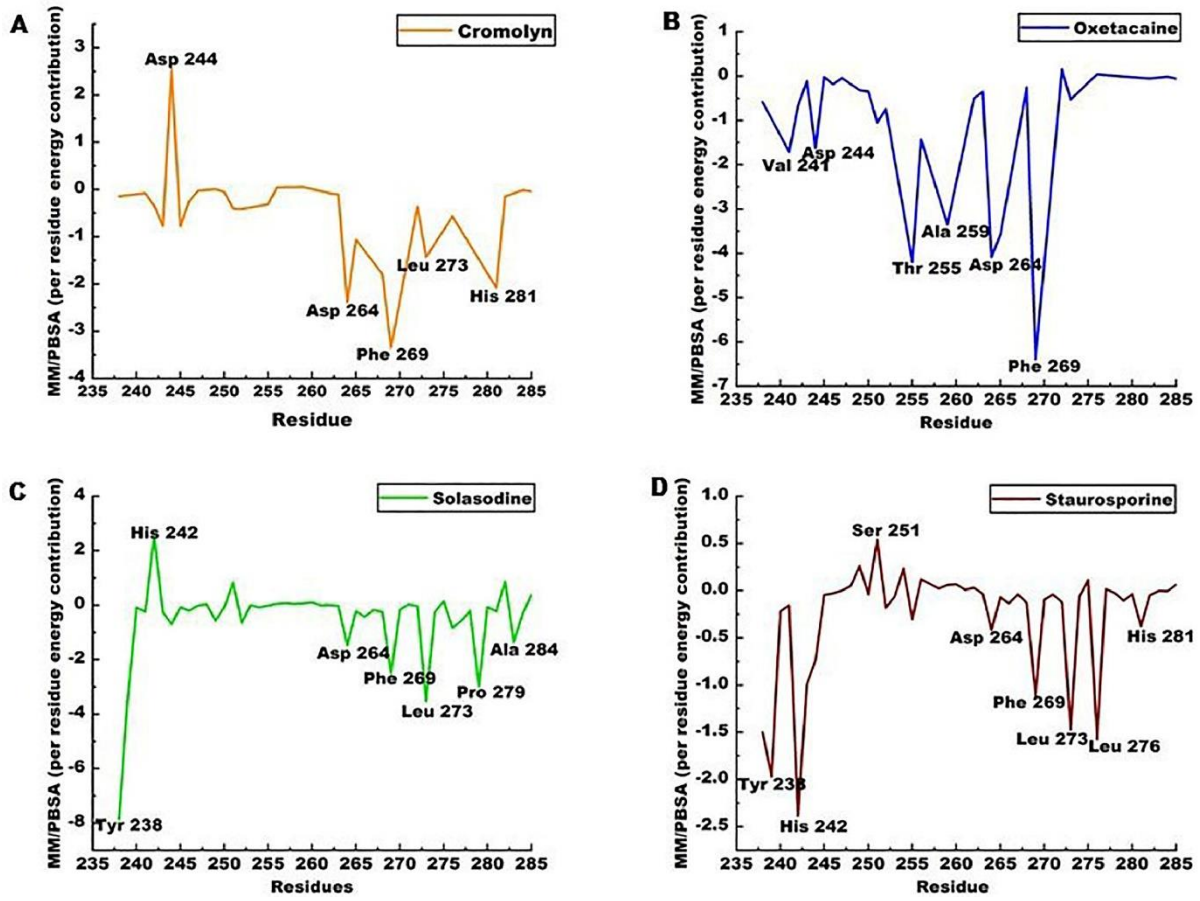

Figure 2.6: Binding energy contribution of complexes.
After the MD simulation, the MM/PBSA approach computed the free binding energy contribution of the protein LdCS's binding site residues with complexes containing (A) Cromolyn, (B) Oxetacaine, (C) Solasodine, and (D) Staurosporine for the 100 ns time period. The primary interacting residues in all complexes were Asp 264, Phe 269, and Leu 273, along with additional residues. Different colors had been used to represent each complex.

The residue present in Cromolyn was Asp 264, Phe 269, Leu 273, and His 281, and in Oxetacaine were Val 241, Asp 244, Thr 255, Ala 259, Asp 264, Pro 265 and Phe 269. This study found that the residue Asp 264, Phe 269, and Leu 273 was essential in ligand binding. Overall, The MM/PBSA binding free energy results were validated with the molecular docking and MD simulation results.

2.3.4 In silico studies with FDA-approved compound database

2.3.4.1 Molecular docking for prediction of efficient inhibitor against Ld citrate synthase

Virtual screening feasibility heavily depends on the identification of a precise binding site, the selection of an appropriate database, and the evaluation of lead molecule pharmacokinetics. The structural requirements of the enzyme's binding pocket and probable ligand-binding sites on the entire protein target can be accurately predicted using molecular docking [Azam et al., 2014]. The docking outcome showed that, as shown in Figure 2.7, all of the investigated ligands had virtually occupied the same location in the protein's binding site. The ideal ligand for the interaction study will have the lowest binding energy and the inhibition constant since it will have the highest ligand and protein binding affinity[Vargas et al., 2018]. Five ligands were selected with a free binding energy between -10 kcal/mol and -12 kcal/mol and compared with the free binding energy of Human citrate synthase. Imatinib fitted on the enzyme's binding pocket and had the lowest binding energy of -11.67 kcal/mol and inhibitor constant (Ki) of 2.79 nM. In contrast, Abemaciclib had the highest binding energy -10.22 kcal/mol and inhibitor constant (Ki) 32.3 nM. The other three, i.e., Bazedoxifene, Vorapaxar, and Amyral, had binding energy -11.02, -10.7, and -10.55 kcal/mol, and inhibitor constant 8.38, 14.26, and 18.55 nM respectively which is shown in Table 2.4. The 2D representation of the docked conformation of the ligand in the binding site of LdCS enzyme was shown in Figure 2.7, which had been done by Discovery studio visualizer. This study was done to find the exact information about the conformation of the ligand in the binding pocket of the Ld citrate synthase enzyme and the significant interaction between them. The important interactions between them are hydrophobic, H-bonding, metal-contact, and π-stacking (π-π T shaped). Abemaciclib, as shown in Figure 2.7 (A), demonstrated hydrophobic interaction with Ala243, Ser251, Ala277, His281, Gly282, Leu283, and Gln286. Besides this interaction, it was involved

Table 2.4: FDA-approved Ligand showing free binding energy (kcal/mol) with LdCS and HsCS and inhibitor constant (Ki) with LdCS.

Ligand Name	Free Binding energy with HsCS (kcal/mol)	Free Binding energy with LdCS (kcal/mol)	The difference in Free Binding energy (kcal/mol)	Inhibitor Constant (Ki) (nm)	Current Application
Imatinib	-7.49	-11.67	4.18	2.79	Chronic myeloid leukemia
Bazedoxifene	-7.69	-11.02	3.33	8.38	Postmenopausal osteoporosis
Vorapaxar	-7.96	-10.7	2.74	14.26	Cardiovascular disease.
Amyral	-7.47	-10.55	3.08	18.55	Control blood sugar level in Type 2 diabetes patients.
Abemaciclib	-5.3	-10.22	4.92	32.3	Breast cancer

in an H-bond interaction where the Nitrogen of the pyridine group interacted with His242, and the Nitrogen of the piperazine groups interacted with Tyr238 & Asn285. Fluorine group interaction with Leu276 and Gly282, Pi-sulfur interaction with Met143, and π-alkyl interaction with Leu276 and Leu283 further stabilized its interaction with its active site. Amyral, as shown in Figure 2.7 (B), had demonstrated hydrophobic interaction with Leu239, Val241, Ala243, His245, Ser251, Ala252, Gly282, and Asn285. This interaction involved H-bond interaction where sulfonyl groups interact with the oxygen of Tyr238 & two different keto groups interact with Asp244 and Asn249. Besides that, Pi-sulfur interaction with Tyr238, Pi-sigma interaction with His242, and π-alkyl interaction with His242 & Leu276 further stabilized its interaction

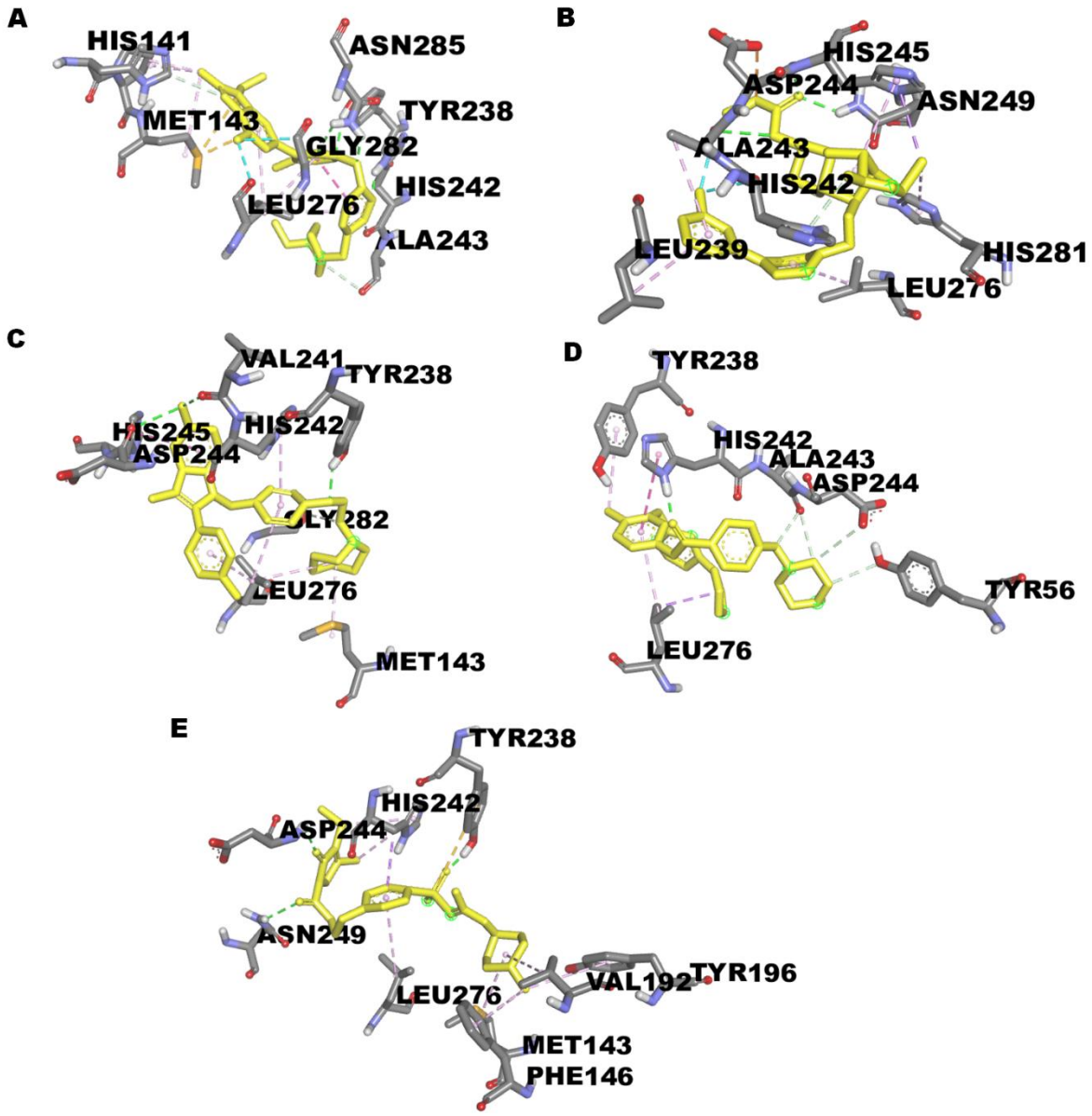

Figure 2.7: Interaction of Protein-ligand complexes.

3D interaction of various ligands **A)** Abemacilcib **B)** Vorapaxar **C)** Bazedoxifene **D)** Imatinib & **E)** Amyral with the amino acid residue of the LdCS binding pocket. Here, the Hydrogen bond had been shown by green, Hydrophobic interaction by different shades of purple, and other interactions, i.e., fluorine and sulfur, had been shown by cyan and orange colour.

with its active site. Bazedoxifene, as shown in Figure 2.7 (C), was in hydrophobic interaction with Ala243, Asn249, Ser251, Phe269, Leu273, His281, and Gly282. Despite this interaction, it involved H-bond interaction where the -OH group interacted with Val241 and Asp244, and ether groups interacted with Tyr238. Besides, π-π T shaped interaction with His245 and π-alkyl

interaction with His242 and Leu276 stabilized its interaction with its binding site. Imatinib, as shown in Figure 2.7 (D), was in hydrophobic interaction with Leu239, Ala243, Asp244, His245, Asn249, Ser251, Ala252, Thr255, Phe269, Leu273, His281, Gly282, and Asn285. Besides hydrophobic interaction, it showed H-bond interaction where the keto group of Imatinib interacted with the Nitrogen of His242. Also, π-π T-shaped interaction with His242, Pi-sigma interaction with Leu276, and Pi-alkyl interaction with Tyr238 stabilized its interaction with its binding site. Vorapaxar, as shown in Figure 2.7 (E), was in hydrophobic interaction with Tyr238, Glu246, Ser251, Ala252, Gly282, and Asn285. It was involved in H-bond interaction where N and O of the carbamate group interact with the oxygen of Ala243, His245, and Asn249. In addition, Fluorine group interaction with His242 & Ala243, Pi-sigma interaction with His245, and π-alkyl interaction with Leu239, Leu276, and His281 further stabilized the interaction with its binding site. In most of the ligand-protein interactions, hydrophobic interaction was found. The hydrophobic inhibitor was found to be better as it would easily fit into the hydrophobic groove of the enzyme and effectively inhibit its activity. The binding pocket's hydrophobicity increases the surface complementarity and compels the inhibitor to maintain a stable conformation [Azam et al., 2014]. H-bond presence further stabilizes the interaction due to the NH and OH groups' fact that they donate and accept the H bond.

2.3.4.2 ADME analysis

The ADMET analysis was done to confirm the efficacy of selected molecules required for designing novel drugs. Five ligands were selected from docking studies based on binding energy, inhibition constant, and hydrogen bond. All Ligands also followed Lipinski's rule of five, which is a rule of a drug to be administered through the oral route [Lipinski, 2004][Bhowmik et al., 2020]. The results are shown in Table 2.2. All ligands with a molecular weight less than 500 Dalton and log P value below five show good permeability across the cell

Table 2.5: Analysis of Lipinski rule of Ligand.

Ligand Name	Property				
	Mass (mg/mol)	**H Acceptor**	**H Donor**	**Log P**	**Refractivity**
Imatinib	493.60	6	2	2.15	154.50
Bazedoxifene	470.60	4	2	3.67	146.97
Vorapaxar	492.58	6	1	4.13	136.05
Amyral	490.62	6	3	2.69	135.17
Abemaciclib	506.59	8	1	2.63	149.17
Miltefosine	408.58	4	1	-0.08	117.43

Note: Lipinksi filter: Mw≤ 500; MLogP ≤ 4.15; N or O ≤ 10; NH or OH ≤ 5.

membrane and have good radial distribution and better absorption. PkCSM software was used for the pharmacokinetics studies of the molecules, which are based on the ADMET properties of the molecules. The absorption studies of all the ligands were done based on the water solubility, Caco-2 permeability, intestinal absorption (human) & skin permeability and compared with the control Miltefosine. The selected ligands had good water solubility as they

had a value below 5. The Caco-2 permeability analysis was done to check the molecules' oral absorption and transport mechanism. All ligands had high Caco-2 permeability as their value was greater than 0.9, except Amyral. All ligands possessed an excellent score of intestinal absorption, indicating that they are highly absorbed in the intestine during oral uptake [Sood et al., 2018]. All ligands and control had good skin permeability as they possessed a skin permeability value less than -2.5. The adsorption analysis of all ligands and its comparison with the control shown in Table 2.6 showed that these drugs had good intestinal absorption and high cellular permeability. In distribution studies, all ligands showed uniform drug distribution in the blood plasma and less unbound fraction, contributing to the good pharmacological properties' distribution. The metabolism of all ligands was studied in which Vorapaxar and Abemaciclib were not a substrate of cytochrome P450. The xenobiotic detoxification was not inhibited as all ligand was not an inhibitor of the main oxidative enzyme cytochrome P450. The excretion studies were done for all ligands. Vorapaxar had the highest, i.e., 1.077 ml/min/kg, Abemaciclib had the lowest, i.e., 0.346 ml/min/kg total clearance value, and the rest of the ligands had values in between, as shown in Table 2.6. The total clearance value is the drug clearance value measured by the combination of hepatic and renal clearance values. It is essential to determine the dose rate to achieve a steady-state concentration. Organic Cation Transporter 2 (OCT2) was responsible for the deposition and renal clearance of xenobiotics compounds. The ligands Bazedoxifene and Imatinib were shown to be renal OCT2 substrates. In contrast, Vorapaxar, Amyral, and Abemaciclib were not a substrate for this uptake transport and did not affect their excretion by the OCT2 pathway and their half-lives. Toxicity studies were also carried out with these ligands, as shown in Table 2.6. AMES test was conducted for the search of mutagenic compounds. Except for Bazedoxifene, no ligand was found to be mutagenic or carcinogenic. There was no ligand found to be an hERG inhibitor.

Table 2.6: ADMET properties analysis of ligands along with the known drugs Miltefosine as a control.

Properties		Ligand Name					Control
		Imatinib	**Bazedoxifene**	**Vorapaxar**	**Amyral**	**Abemaciclib**	**Miltefosine**
ABSORPTION	Water Solubility (Log mol/L)	-3.379	-4.026	-3.777	-4.199	-2.943	-5.792
	Caco2 Permeability (log Papp in 10^{-6} cm/s)	0.997	1.1	1.134	0.613	1.584	1.035
	Intestinal Absorption (% Absorbed)	93.146	91.397	95.232	65.49	87.2	87.367
	Skin Permeability Log Kp	-2.736	-2.736	-3.707	-2.921	-2.735	-2.733
DISTRIBUTION	VDss (human) (log/kg)	1.586	0.168	0.054	-0.761	0.402	0.306
	Fraction unbound (human) (Fu)	0.084	0.237	0.279	0.179	0.352	0.171
METABOLISM	CYP Substrate	Yes	Yes	No	Yes	No	Yes
	CYP Inhibitor	No	No	No	No	No	No
EXCRETION	Total Clearance (Log ml/min/kg)	0.758	0.787	1.077	0.606	0.346	1.156
	Renal OCT2 Substrate	Yes	Yes	No	No	No	No
TOXICITY	AEMS Toxicity	No	Yes	No	No	No	No
	Max. tolerated dose (Human) (Log mg/kg/day)	0.341	0.521	-0.081	-0.303	0.292	0.388
	hERG inhibitor	No	No	No	No	No	No
	Hepatotoxicity	Yes	No	No	Yes	No	No
	Skin Sensitisation	No	No	No	No	No	No

Note: Water solubility < 5; Caco2 > 0.90; Intestinal absorption > 30%; Skin permeablity (log Kp) < -2.5; VDss is low if logVDss < -0.15 and high if log VDss > 0.45; MRTD ≤ 0.477 log(mg/kg/day) is low while > 0.477 log(mg/kg/day) is high.

hERG is a gene that codes a potassium ion channel protein and contributes to the coordination of the heart's beating. Except for Imatinib and Amyral, no ligand was hepatotoxic. Any ligand did not show skin sensitization properties.

3.3.3.3 Molecular Dynamic Simulation Analysis

MD simulations were performed up to 100 ns to understand the stability of the interaction between Ligand and Ld citrate synthase. RMSD analysis is an important analysis of MD simulation by which able to understand the structural stability of the protein and complexes with time. This analysis was done for both apoprotein and protein-ligand complexes for 100 ns trajectory, and the graph was generated. The RMSD of the backbone atom of Ld citrate synthase and the protein-ligand complex graph was shown in Figure 2.8 (A) found that the Ld citrate synthase had RMSD 0.7 nm and showed convergence from 30 ns with slight fluctuation near 70 ns. The complex Imatinib and Abemaciclib had RMSD 0.9 nm. The Imatinib fluctuated till 40 ns and Abemaciclib till 25 ns; after that, it became stable and showed steady flow. The complex Bazedoxifene and Vorapaxar had RMSD 0.8 nm and became stable after 15 ns, whereas the complex Amyral had RMSD 0.7 nm and showed a steady pattern after 5 ns, but slight fluctuation was observed near 25 ns. The ligand RMSD graph was also plotted, shown in Figure 2.8 (B). The ligands Abemaciclib, Amyral, and Vorapaxar had RMSD 0.3 nm, 0.35 nm, and 0.4 nm, respectively, showing the most stable plot. There was no fluctuation observed. The ligand Bazedoxifene had RMSD 0.25 nm and became stable after 20 ns, whereas the complex Imatinib had RMSD 0.3 nm and became stable after 45 ns. The RMSD of the ligand in every complex was less than 4 Å, while the RMSD of the backbone atom was less than 9Å, demonstrating the ligand's remarkable stability in the protein binding pocket [Kuldeep et al., 2020]. Abemaciclib, Amyral, Bazedoxifene, Imatinib, and Vorapaxar were used in RMSF analysis of 308 residues of Ld citrate synthase and protein-ligand complex to understand the flexibility of each residue [Raj et al., 2019b]. The RMSF graph, which is in Figure 2.8 (C),

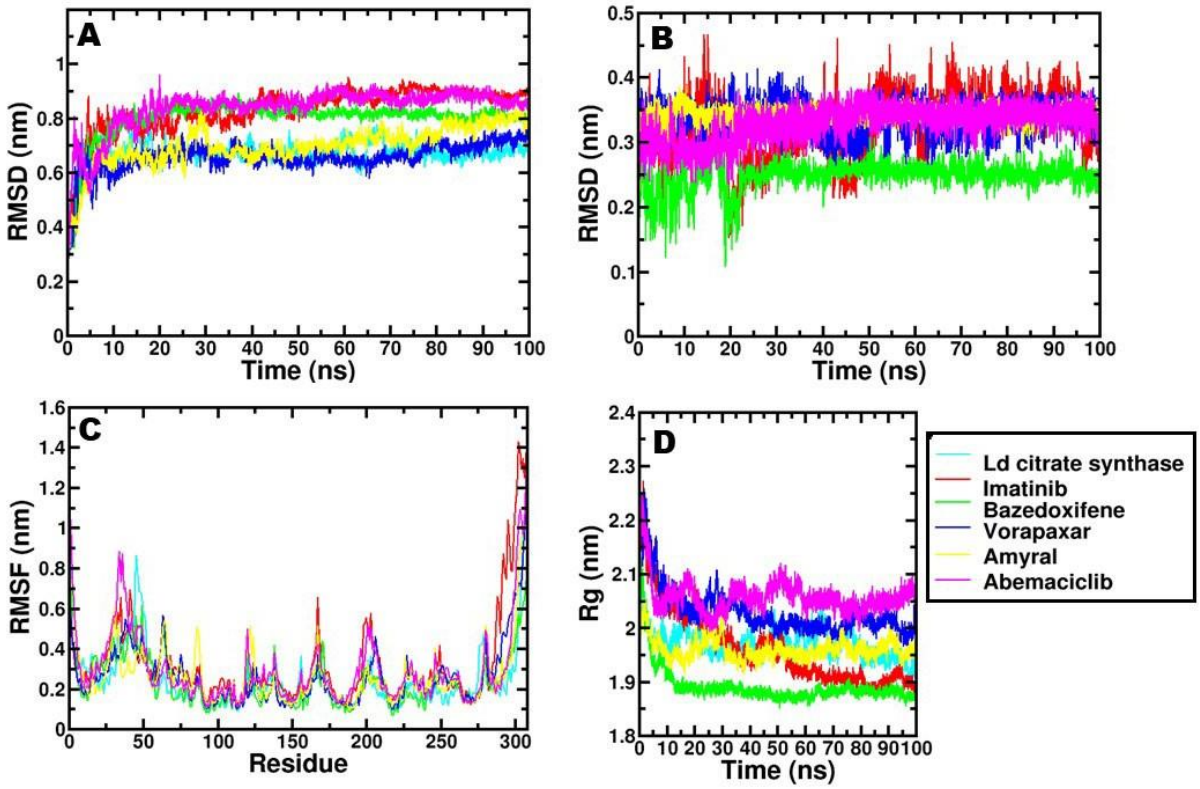

Figure 2.8: Molecular Dynamic Simulation analysis of LdCS and Complexed ligands, i.e., Imatinib, Bazedoxifene, Vorapaxar, Amyral, and Abemacilcib that performed for 100 ns of time duration. (A) RMSD plot of the backbone atom of LdCS protein and complexed ligands. **(B)** RMSD plot of ligands complexed with LdCS protein. **(C)** RMSF plot of all 308 residues of LdCS protein and complexed ligands. **(D)** Rg plot of the backbone atom of LdCS protein and complexed ligands. Each complex was shown in a different color**.**

displayed the major fluctuation in the N and C terminal portions of Ld citrate synthase and all protein-ligand complexes, which may be caused by the presence of loops and low, stable beta sheets in these regions of the protein [Kuldeep et al., 2020]. The binding and active site region is very compact & rigid, and stable in the dynamic environment, as evidenced by the RMSF value of the residues implicated in the active and binding site region being less than 0.4 nm and the reduced fluctuation observed in all protein-ligand complexes [Bhowmik et al., 2020]. In an MD simulation, the protein complex's compactness and fluctuation are depicted by the radius of gyration [Bhowmik et al., 2020][Freitas et al., 2018]. This analysis demonstrates the folding and unfolding of polypeptide chains or the various protein conformations [Samuel Singh, 2019]. The radius of gyration studies was done for Ld citrate synthase and protein-ligand

complex, i.e., Abemaciclib, Amyral, Bazedoxifene, Imatinib, and Vorapaxar, estimated the mass of atoms relative to the center of the complex's mass. The radius of the gyration graph was shown in Figure 2.8 (D), which showed that most of the complex was more stable than apoprotein. The Rg value of Ld citrate synthase was 2.05 nm and had slight fluctuation throughout. The complex Vorapaxar and Amyral had an Rg value of 1.95 nm and showed stability after 15 ns, but in the case of Amyral, little fluctuation was observed between 20 ns to 30 ns. The other complexes, i.e., Imatinib, Bazedoxifene, and Abemaciclib, had an Rg value of 1.9 nm and showed stability in the case of Imatinib and Bazedoxifene after 15 ns whereas in the case of Abemaciclib after 30 ns. The Rg value of all complexes was very near to the Rg value of Ld citrate synthase, which showed that all complexes had formed a stable and rigid bond.

Hydrogen bond analysis between Ld citrate synthase and ligand was done for a period of 100 ns simulation, and the involvement of binding site residue in bond formation was also analyzed. The graph is shown in Figure 2.9. The only complex with a maximum of seven hydrogen bonds and an average of four hydrogen bonds was amyral. Hydrogen bonds were formed by the binding pocket residues Tyr238, His242, Ala243, His245, His281, Gly282, Ala284, and Asn285. Imatinib's complex maintained an average hydrogen bond number of four while reaching a high of six. With binding site residues like Tyr238, His242, Ala243, His245, Gly247, Asn249, Ser251, Thr255, His281, Ala284, and Asn285, this complex had also created a hydrogen bond. The complex Abemaciclib produced a maximum of three hydrogen bonds, with an average of two. Tyr238, His242, Ala284, and Asn285 residues, which are important in binding to the active site of the Ld citrate synthase protein, had formed a hydrogen bond with this complex. The Bazedoxifene and Vorapaxar complexes had generated a maximum of five and four hydrogen bonds, respectively, with an average of two hydrogen bonds still present. These complexes had not formed a hydrogen bond with the binding site residue of Ld citrate

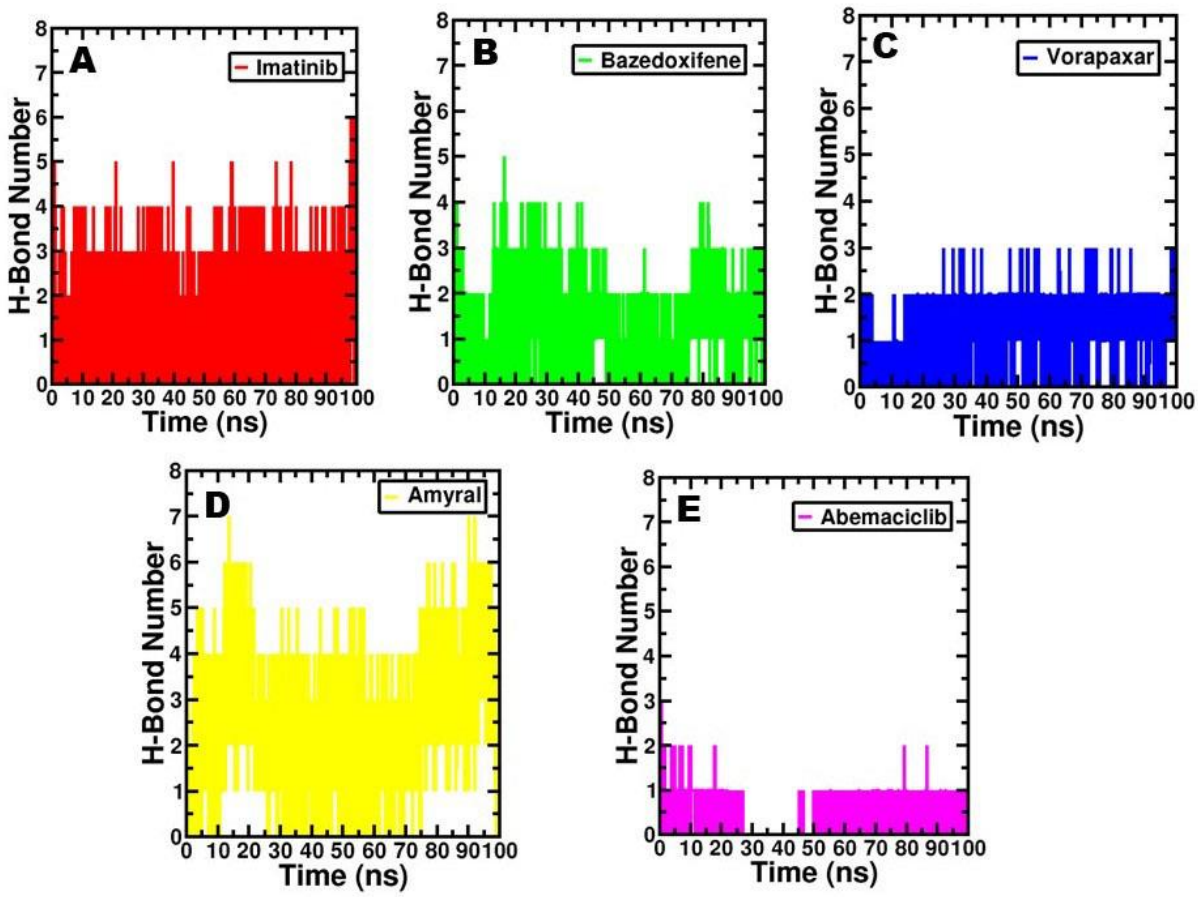

Figure 2.9: Hydrogen bond analysis
The creation of hydrogen bonds between the LdCS protein and the ligands imatinib, bazedoxifene, vorapaxar, amyral, and abemaciclib throughout the course of a 100 ns MD simulation. Amyral had the highest number of H-bonds, seven, whereas Abemaciclib had the lowest number of H-bonds, one. The H-bond counts for the other ligands ranged from six to five to three, respectively. Different colors had been used to indicate each complex.

synthase protein, while these were stable and observed within the pocket during the 100 ns of simulation. Therefore, the binding affinities of these complexes, along with other complexes, were analyzed by calculating the binding free energy, which is the average of electrostatic, Vander Waals, polar solvation, and SASA energy. A few key residues, i.e., Tyr238, His242, and His245, were found that were commonly involved in hydrogen bond formation between ligand and binding site residue of Ld citrate synthase protein in both docking and MD Simulation. The molecular mechanics Poisson-Boltzmann surface area (MM-PBSA), besides MD simulation, is one of the most widely used methods for the calculation of binding affinities and also the rescoring of the docked complexes, which help in the selection of the best drug

Table 2.7: Calculation of average binding energy of different complexes with Ld citrate synthase after MD simulation.

Ligand Name	Vander Waal Energy (kJ/mol)	Electrostatic Energy (kJ/mol)	Polar Solvation Energy (kJ/mol)	SASA Energy (kJ/mol)	Binding Energy (kJ/mol)
Vorapaxar	-252.95	-12.00	69.36	-26.08	-221.68
Abemaciclib	-218.45	-2.30	37.93	-20.65	-203.47
Bazedoxifene	-61.46	-179.16	75.82	-6.54	-171.34
Imatinib	-179.20	-469.61	620.73	-19.79	-47.87
Amyral	-62.25	-16.14	43.01	-5.64	-41.02

molecule [Freitas et al., 2018]. In the calculation of free binding energy, four individual energy components were involved. The free binding energy was calculated for all protein-ligand complexes and is shown in Table 2.7. The complexes Vorapaxar, Abemaciclib, and Bazedoxifene had the lowest binding energy, -221.68 kJ/mol, -203.47 kJ/mol, and -171.34 kJ/mol, whereas the complexes Imatinib and Amyral had the binding energy -47.87 kJ/mol and -41.02 kJ/mol respectively. The energy component favorably involved in binding energy formation was Vander Waals, electrostatic and polar solvation, whereas unfavorably involved one was SASA or nonpolar solvation. Vander Waals energy was the major contributing energy in Abemaciclib, Vorapaxar, and Amyral. In Bazedoxifene, the electrostatic energy and In Imatinib, Polar Solvation energy was the main contributing energy. Changes in each residue's

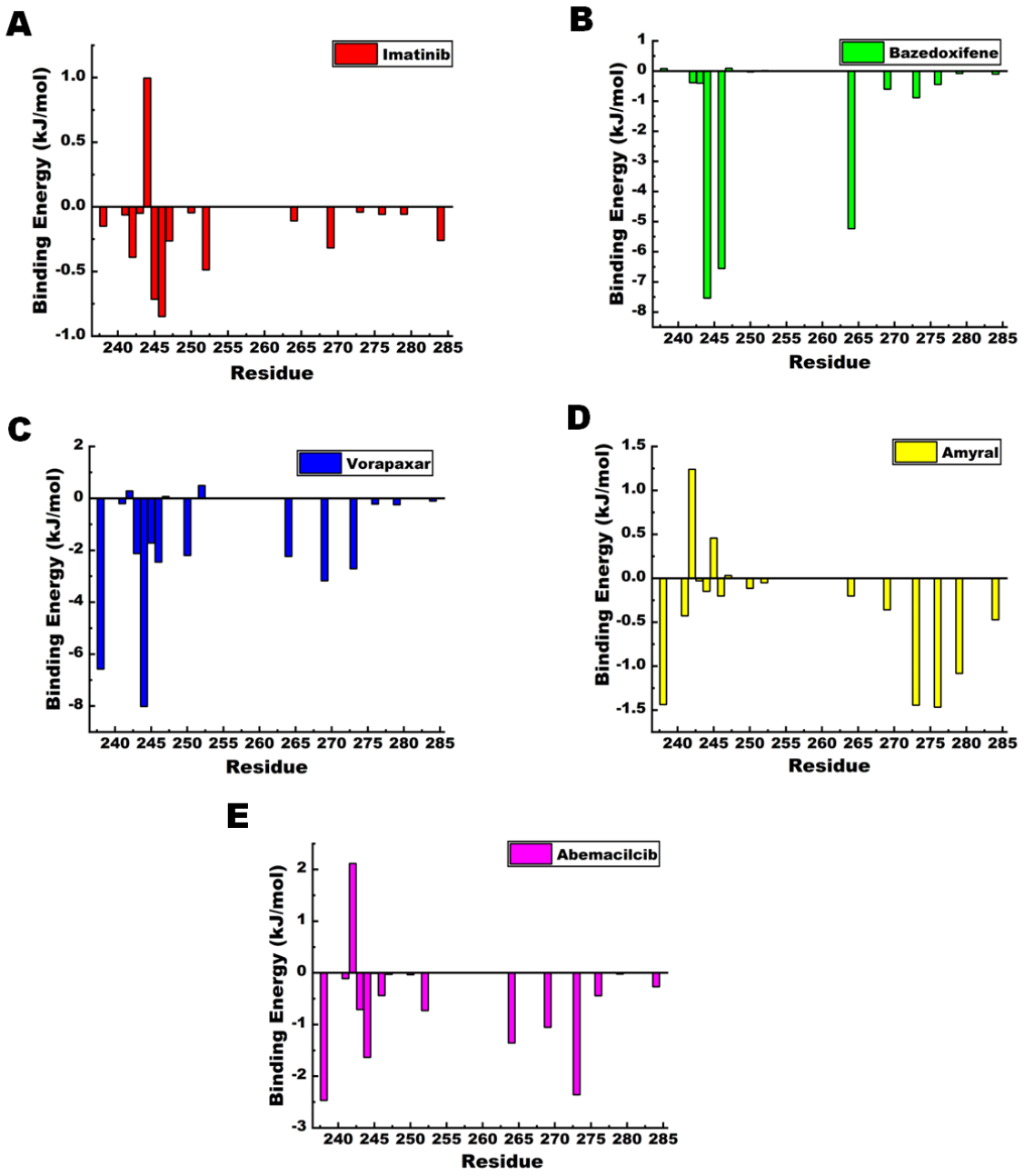

Figure 2.10: The Free binding energy contribution analysis of complexes. The free binding energy contribution of major residues of Protein-ligand complexes **(A)** Imatinib, **(B)** Bazedoxifene, **(C)** Vorapaxar, **(D)** Amyral, and **(E)** Abemaciclib in bond formation during 100 ns of MD simulation, which was identified by the MM/PBSA methods. Different colors have demonstrated various complexity.

energy contribution were a key contributor to the variation in free-binding energy. The same binding pocket of the enzymes had, however, hosted all of the complexes. In order to determine the energy contribution of each residue in binding at the protein's active site, as well as in the investigation of residues involved in interactions other than hydrogen bonds for stability,

energy decomposition studies for all protein-ligand complexes, as shown in Figure 2.10, were conducted [V. M et al., 2018]. Tyr238, Val241, His242, Ala243, Asp244, Glu246, Asp264, Phe269, Leu273, Leu276, and Asn285 were the main active site residues involved in Vander Waal and electrostatic interaction in all complexes. Each complex had a varied contribution from the binding energy of each residue, which significantly altered the total binding energy of each complex. Although there isn't a significant hydrogen bond interaction, the complex's stability can be explained by the larger energy contribution from the binding site residues in the instance of the complex Bazedoxifene and Vorapaxar.

2.4 Discussion

Leishmaniasis, the second most common tropical illness in the world after malaria, causes more than 30,000 fatalities each year. Chemotherapy is the only treatment for the condition at this time because there is no vaccination [Sangshetti et al., 2015]. At the moment, there aren't many medications available to treat this disease [Singh et al., 2012]. An effective antileishmanial medication that is low in toxicity, affordable, and highly efficacious is thus urgently needed. To develop a potent inhibitor against it, a workable technique would be to comprehend host-parasite interaction and the level of host homology. Citrate synthase is an enzyme that participates in the biosynthesis of lipids, proteins, and nucleotides that Leishmania needs for pathogenicity, growth, and defense [Saunders et al., 2011]. This enzyme was targeted based on its functionality, and its model was generated using the ITASSER server. This model served as the basis for docking studies with 1565 FDA-approved drugs and 1055 natural compounds sourced from the ZINC database, aiming to identify potential compounds for LdCS. From the FDA-approved drug database, the top five hits—Imatinib, Bazedoxifene, Vorapaxar, Amyral, and Abemaciclib—were selected, along with the top four hits—Staurosporine, Solasodine, Cromolyn, and Oxetacaine—from the natural compound database. These hits exhibited binding energies ranging from -9 kcal/mol to -12 kcal/mol. Although the natural compounds showed

slightly higher binding energies compared to FDA-approved compounds, they demonstrated interaction with the enzyme's active site residues. Notably, all selected molecules adhered to Lipinski's rule with zero violations, which assesses the oral activity of drugs. These ligands were then used for MD Simulation and MM-PBSA investigations since docking estimates free binding energy based on expected binding poses, necessitating the necessity for MD Simulation research. Based on RMSD, RMSF, Radius of gyration, and Hydrogen bond analysis, MD simulation investigations were carried out. Protein-ligand complexes' structural stability, lack of fluctuation in their catalytic area, and compactness demonstrated that these ligands would interact with proteins in a stable and robust manner at their binding sites [Kuldeep et al., 2020] [Bhowmik et al., 2020] [Freitas et al., 2018]. All ligands had formed hydrogen bonds, but Amyral had formed the highest seven hydrogen bonds with continuity of four hydrogen bonds. Based on the distinction between the final free binding energies of bound and unbound complexes, MM-PBSA investigations were conducted to examine the variation in binding energy following MD simulation. Additionally, it would aid in the distinction between active and inactive medications based on docking score [Good, 2006]. Oxetacaine demonstrated the strongest hydrophobic contacts in this investigation, followed by Vorapaxar, Abemacilcib, Bazedoxifene, and Solasodine, which were assessed based on binding energy. The other complexes like Staurosporine, Imatinib, Cromolyn, and Amyral also had comparable free binding energy. Per residue, energy decomposition studies were also carried out and found that a few residues like Try 238, His 242, His 245, Asp 264, Phe 269, Leu 273, and Asn 285 were commonly involved in interaction with the active site of LdCS and comparable with docking result which taken for pharmacokinetics studies based on ADMET characteristics using PkCSM server. These investigations were required because inadequate pharmacokinetics play a major role in the majority of drug development failures, and also, it becomes crucial because the majority of the clinical trial experiments are expensive & involve animals, which raises

moral dilemmas. All selected ligands exhibited good water solubility and strong CaCO-2 permeability as their values are less than 5 and larger than 0.9. all ligands had good intestinal absorption scores, which meant that during oral uptake, they were extensively absorbed in the gut. There were no skin sensitivity issues arises and their values were below -2.5, all ligands exhibited good skin permeability. They also demonstrated a more consistent medication distribution in the blood plasma and a lower level of unbound fraction. Since these ligands did not inhibit P450, xenobiotic detoxification was not hampered. Together, they have little toxicity, adequate metabolism, and good absorption, solubility, and permeability [Bhowmik et al., 2020]. it is hoped that the proposed ligand would be a strong inhibitor of Ld citrate synthase and a potential drug for Leishmaniasis.

2.5 Conclusion

The present study employed an *in-silico* drug repurposing strategy to identify a selective inhibitor for *L. donovani* citrate synthase. Through molecular docking with both LdCS and HsCS, along with subsequent molecular dynamic simulation and MMPBSA analysis, five compounds—Abemaciclib, Bazedoxifene, Imatinib, Vorapaxar, and Amyral—were identified. These compounds formed the most stable complexes with the protein's active site and exhibited the lowest binding energies. However, further investigation, including *in vitro* and *in vivo* analyses, is necessary to validate these ligands as the safest and most effective treatment for leishmaniasis. Consequently, the proposed ligands hold promise as prospective antileishmanial drugs for future development.